

Disease-Atlas: Navigating Disease Trajectories using Deep Learning

Bryan Lim and Mihaela van der Schaar

Abstract—Joint models for longitudinal and time-to-event data are commonly used in longitudinal studies to forecast disease trajectories over time. While there are many advantages to joint modeling, the standard forms suffer from limitations that arise from a fixed model specification, and computational difficulties when applied to high-dimensional datasets. In this paper, we propose a deep learning approach to address these limitations, enhancing existing methods with the inherent flexibility and scalability of deep neural networks, while retaining the benefits of joint modeling. Using longitudinal data from two real-world medical datasets, we demonstrate improvements in performance and scalability, as well as robustness in the presence of irregularly sampled data.

I. INTRODUCTION

BUILDING a Disease Atlas for clinicians involves the dynamic forecasting of medical conditions based on clinically relevant variables collected over time, and guiding them in charting a course of action. This includes the simultaneous prediction of survival probabilities, risks of developing related diseases, and relevant biomarker trajectories at different stages of disease progression. While prognosis, i.e. survival predictions, is usually the main area of focus [1], [2], a growing area in precision medicine is the forecasting of personalized disease trajectories, using patterns in temporal correlations and associations between related diseases to predict their evolution over time. [3], [4]. Dynamic prediction methods that account for these interactions are particularly relevant in multimorbidity management, as patients with one chronic disease typically develop other long-term conditions over time [5]. With the mounting evidence on the prevalence of multimorbidity in ageing populations around the world [6], the ability to jointly forecast multiple clinical variables would be beneficial in providing clinicians with a fuller picture of a patient’s medical condition.

Joint models for longitudinal and time-to-event data are commonly used in studies where longitudinal biomarkers may be highly associated with an event of interest. Using individual models for each data trajectory as building blocks, such as linear mixed models for longitudinal data and the Cox proportional hazard model for survival, joint models add a common association structure on top of them, e.g. through shared-random effects or frailty models [7]. From a dynamic prediction perspective, joint models have been shown to lead to a reduced bias in estimation [8] and improved predictive

accuracy [9]. However, standard joint models face severe computational challenges when applied to large datasets, which arise when increasing the dimensionality of the random effects component [7].

To overcome the limitations of joint models, we introduce Disease-Atlas - a scalable deep learning approach to forecasting disease trajectories over time. Our main contributions are as follows:

a) Deep Learning for Joint Models: We provide a novel conception of the joint modeling framework using deep learning, capturing the relationships between trajectories through shared representations learned directly from data, and improving scalability as a whole. In addition, the network outputs parameters of predictive distributions for longitudinal and time-to-event data that take a similar form to the sub-models used in joint modeling.

b) Robustness to Irregular Sampling via Multitask Learning: Observations in Electronic Health Records (EHRs) are very rarely aligned at every time step, as measurements can be collected at irregular time intervals. Training a multioutput neural network on EHRs would require the imputation of the target labels as a pre-processing step, so as to artificially align the dataset prior to calibration. This could lead to poorer predictions if imputation quality is low, as the network is trained to reproduce the imputed label as opposed to the predicting true value of the observation. To mitigate this issue, we formulate joint model calibration as a multitask learning problem, grouping variables, which are measured at the same time and with similar sampling frequencies, together into tasks, and training the network using only actual observations as target labels.

c) Incorporating Medical History into Forecasts: While deep learning for medicine has gained popularity in recent times, the majority of methods, such as [10], [11], only use covariates at a single time point in making predictions. However, a patient’s medical history could also be informative of her future clinical outcomes, and predictions could be improved by incorporating past information. We integrate historical information into our network using a Recurrent Neural Network (RNN) in the base layer, which dynamically updates its memory state over time.

II. RELATED WORK

While the utility of joint models has been demonstrated by its popularity in longitudinal studies, numerous modelling choices exist - each containing their own advantages and limitations (see [7] for a full overview). [12], for example,

B. Lim and M. van der Schaar are with Department of Engineering Science, University of Oxford, Oxford, United Kingdom (email: bryan.lim@eng.ox.ac.uk, mihaela.vanderschaar@eng.ox.ac.uk). This work is supported by the UK Cystic Fibrosis Trust and the Oxford-Man Institute.

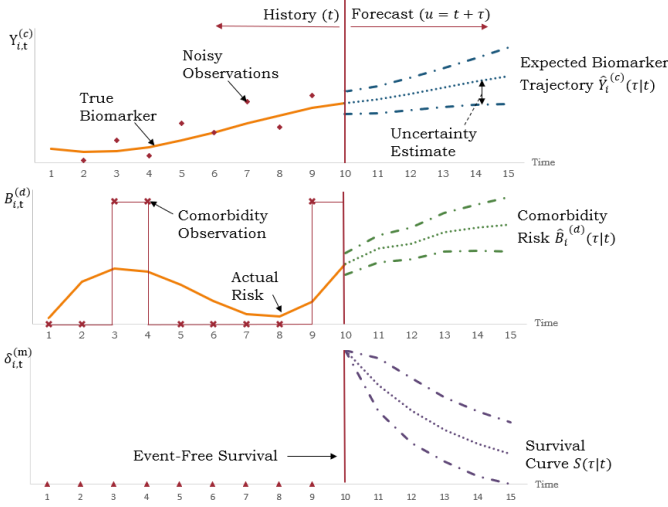


Fig. 1. Illustration of Dynamic Prediction with Joint Models

highlight the sensitivity of predictions to the association structures used, adopting a Bayesian model averaging approach instead to aggregate the outputs of different models over time. In this respect, the flexibility of deep learning has the potential to enhance dynamic predictions with joint models, by directly learning variable relationships from the data itself, and completely removing the need for explicit model specification. In addition, [7], [13], [14], [15] note performance limitations when applying standard joint models to high-dimensional datasets. These are typically estimated using Monte Carlo Expectation Maximization (MC-EM) or Markov Chain Monte Carlo (MCMC) sampling methods, which rapidly grow in complexity with the number of covariates and random effects. As such, most studies and software packages often focus on modelling a single or a small number of longitudinal measurements, along with a time-to-event of interest. However, the increase in data availability through electronic health records opens up the possibility of using information from multiple trajectories to improve predictions. Recent works have attempted to address this limitation by exploiting special properties of the longitudinal submodels, such as the multivariate skew-normal structure in [16], and the combination of variational approximation and dynamic EM-style updates over time in [15]. As such, the use of deep learning holds much promise in enhancing the performance of joint models, given its inherent ability to scale with large datasets without the need for specific modeling assumptions.

Deep learning has seen increasing use in medical applications, with successes in traditional survival analysis [11], [17] survival analysis with competing risks [18], [10] and treatment recommendations [19]. In general, these methods focus purely on forecasting survival, do not consider dynamic prediction over time and only use covariates at a single time point in making predictions. Deep Kalman Filters [20] use a network which does dynamically update its latent states over time but assumes that all outputs follow the same distribution. This prevents it from being applied to heterogeneous datasets, which limits its

usage for joint modeling. To the best of our knowledge, this paper is the first to investigate the use of deep learning in joint models for longitudinal and survival trajectories.

Multitask learning has also been explored in other deep learning methods applied to medicine, such as in diagnosing Alzheimer’s Disease [21], and predicting outcomes of hospitalized patients [22]. Using images from MRI and CT scans, [21] apply multitask learning to enhance the representations learnt by the network, predicting the patient label along with 2 other cognitive scores. [22], on the other hand use, use LSTMs with multitask learning across a large number of hospital prediction tasks, such as in-hospital mortality, decompensation, and length of stay. While both these networks bear resemblance to our model, a few key differences exist. First, we apply multitask learning to reduce estimation errors that arise from irregular sampling in our dataset, by training the network only on actual observations. Next, the application of Monte Carlo (MC) dropout in our network allows us to generate uncertainty estimates for our forecasts, while their networks only use point estimates. Moreover, their networks consider predictions only at fixed time points (either at the end of a sequence or one prediction per time step), while we produce forecasts at arbitrary points in the future, through the specification of a flexible predictive horizon in the task-specific layer. [21] also do not incorporate full historical information, using only scans at individual time steps to make predictions.

III. PROBLEM DEFINITION

For a given longitudinal study, let there be N patients with observations made at time t , for $0 \leq t \leq T_{cens}$ where T_{cens} denotes an administrative censoring time¹. For the i^{th} patient at time t , observations are made for a K -dimensional vector of longitudinal variables $\mathbf{V}_{i,t} = [Y_{i,t}^{(1)}, \dots, Y_{i,t}^{(C)}, B_{i,t}^{(1)}, \dots, B_{i,t}^{(D)}]$, where $Y_{i,t}^{(c)}$ and $B_{i,t}^{(d)}$ are continuous and discrete longitudinal measurements respectively, a L -dimensional vector of external covariates $\mathbf{X}_{i,t} = [X_{i,t}^{(1)}, \dots, X_{i,t}^{(L)}]$, and a M -dimensional vector of event occurrences $\delta_{i,t} = [\delta_{i,t}^{(1)}, \dots, \delta_{i,t}^{(M)}]$, where $\delta_{i,t}^{(m)} \in \{0, 1\}$ is an indicator variable denoting the presence or absence of the m^{th} event. $T_{i,t}^{(m)}$ is defined to be the first time the event is observed after t , which allows it to model refer to both repeated events, and events that lead to censoring (e.g. death). The final observation for patient i occurs at $T_{i,max} = \min(T_{cens}, T_{i,0}^{(a_1)}, \dots, T_{i,0}^{(a_{max})})$, where $\{a_i, \dots, a_{max}\}$ is the set of indices for events which censor observations. Furthermore, we introduce a filtration $\mathcal{F}_{i,t}$ to capture the full history of longitudinal variables, external covariates and event occurrences of patient i until time t .

A. Joint Modeling

From [7], numerous sub-models for longitudinal measurements exist, each with their own pros and cons. General forms for continuous and binary longitudinal measurements are typically expressed as:

$$Y_{i,u}^{(c)} | \mathcal{F}_{i,t} \sim \mathcal{N} \left(m^{(c)} \left(u, \mathcal{F}_{i,t}; \mathbf{b}_i, \tilde{\mathbf{W}} \right), \sigma_u^{(c)2} \right) \quad (1)$$

¹ Administrative censoring refers to the right-censoring that occurs when a study observation period ends.

$$B_{i,u}^{(d)} | \mathcal{F}_{i,t} \sim \text{Bernoulli} \left(\Phi^{(d)} \left(u, \mathcal{F}_{i,t}; \mathbf{b}_i, \tilde{\mathbf{W}} \right) \right) \quad (2)$$

Where $m^{(c)}(\cdot)$ is a function for the predictive mean of the c -th longitudinal variable, and $\sigma_t^{(c)2}$ its variance. $\Phi^{(d)}(\cdot)$ is a function for the probability of the binary observation, such as the commonly used logit or probit functions, and $\tilde{\mathbf{W}}$ is the vector of static coefficients used by the sub-models.

In both models, \mathbf{b}_i is a vector of association parameters used across trajectories, and define the association structure of the joint model. While the majority of models use subject-specific random effects, this can also refer to time-dependent latent variables as seen in [23] or shared spline coefficients in [16].

Event times can be expressed using the general form below:

$$T_{i,t}^{(m)} | \mathcal{F}_{i,t} \sim \mathcal{S} \left(\Lambda^{(m)} \left(t, \mathcal{F}_{i,t}; \mathbf{b}_i, \tilde{\mathbf{W}} \right) \right) \quad (3)$$

Where \mathcal{S} is an appropriate survival distribution (e.g. Exponential, Weibull etc), and $\Lambda^{(m)}(\cdot)$ is a generic cumulative hazard function. In most joint model applications, this typically takes the form of the Cox proportional hazards model.

The standard linear mixed effects models can be expressed as:

$$\begin{aligned} Y_{i,t}^{(c)} &= \mathbf{X}_{i,t}^\top \theta_{fix}^{(c)} + \mathbf{R}_{i,t}^\top \theta_{rand}^{(c)} + \epsilon_{i,t}^{(c)} \\ &= m^{(c)}(t) + \epsilon_{i,t}^{(c)} \end{aligned} \quad (4)$$

$$h_{i,t}^{(m)} = h_0(t) \exp \left(\mathbf{B}_i^\top \gamma^{(m)} + \beta^{(m)} m^{(c)}(t) \right) \quad (5)$$

Where $X_{i,t}$ and $R_{i,t}$ are time-dependent design vectors for fixed effects $\theta_{fix}^{(c)}$ and random effects $\theta_{rand}^{(c)}$, $\epsilon_{i,t} \sim N(0, \sigma_t^{(c)2})$ is a random noise term, and $h_{i,t}$ is the hazard rate of the survival process, with patient fixed covariates \mathbf{B}_i and static coefficient $\beta^{(m)}$.

In this model, we define the association parameters of the joint model to be those common to both longitudinal and survival processes, i.e $\mathbf{b}_i = [\theta_{fix}^{(c)}, \theta_{rand}^{(c)}]$, and static coefficients which are unique to the separate processes, i.e. $\tilde{\mathbf{W}} = [\gamma^{(m)}, \beta^{(m)}]$.

B. Dynamic Prediction

Dynamic prediction in joint models can be defined as the estimation of both the expected values of longitudinal variables and survival probabilities over a specific time window τ in the future:

$$\hat{V}_i^{(k)}(\tau|t) = \mathbb{E} \left[V_{i,t+\tau}^{(k)} | \mathcal{F}_{i,t}; \mathbf{b}_i, \tilde{\mathbf{W}} \right] \quad (6)$$

$$\begin{aligned} S_i^{(m)}(\tau|t) \\ = P \left(T_{i,0}^{(m)} \geq t + \tau | T_{i,0}^{(m)} \geq t, \mathcal{F}_{i,t}; \mathbf{b}_i, \tilde{\mathbf{W}} \right) \end{aligned} \quad (7)$$

Where $V_{i,t}^{(k)}$ is the k^{th} longitudinal variable at time t that can be either continuous or binary. A conceptual illustration of dynamic prediction can be found in Figure 1. For continuous longitudinal variables, such as biomarker predictions, the goal is to forecast its expected value given all the information until the current time step (i.e. $\mathcal{F}_{i,t}$). In the case of binary observations, such as the presence of a comorbidity, the expectation in Equation 6 is the probability (or risk) of developing a comorbidity at time $t + \tau$. The survival curves

shown give us the probability of not experiencing an event over various horizons τ given $\mathcal{F}_{i,t}$. While the uncertainty estimates are model dependent, these are usually expressed via confidence intervals in frequentist methods, or using the posterior distributions for $\mathbf{b}_{i,t}$ and $\tilde{\mathbf{W}}$ in Bayesian models.

IV. NETWORK DESIGN

A. Architecture

Disease-Atlas captures the associations within the joint modeling framework, by learning *shared representations* between trajectories at different stages of the network, while retaining the same sub-model distributions seen in joint models. The network, as shown in Figure 2, is conceptually divided into 3 sections: 1) A shared temporal layer to learn the temporal and cross correlations between variables, 2) task-specific layers to learn shared representations between related trajectories, and 3) an output layer which computes parameters for predictive sub-model distributions for use in likelihood loss computations during training and generating predictive distributions at runtime.

The equations for each layer are listed in detail below. For notational convenience, we drop the subscript i for variables in this section, noting that the network is only applied to trajectories from one patient at time.

a) *Shared Temporal Layer*: We start with an RNN at the base of the network, which incorporates historical information (i.e. \mathcal{F}_t) into forecasts by updating its memory state over time. For the tests in Section V, the usage of both the Simple Recurrent Network (SRN) and LSTM in this layer was compared.

$$[\mathbf{h}_t, \mathbf{m}_t] = \text{RNN}([\mathbf{X}_t, \mathbf{V}_t], \mathbf{m}_{t-1}) \quad (8)$$

Where \mathbf{h}_t is the output of the RNN and \mathbf{m}_t its memory state. To generate uncertainty estimates for forecasts and retain consistency with joint models, we adopt the MC dropout approach described in [24]. Dropout masks are applied to the inputs, memory states and outputs of the RNN, and are also fixed across time steps. For memory updates, the RNN uses the Exponential Linear Unit (ELU) activation function.

b) *Task-specific Layers*: For the task-specific layers, variables are grouped according to the sub-model types in Section III-A, with layer $\mathbf{z}_{c,t}$ for continuous-valued longitudinal variables, $\mathbf{z}_{b,t}$ for binary longitudinal variables and $\mathbf{z}_{e,t}$ for events. Dropout masks are also applied to the outputs of each layer here.

$$\mathbf{z}_{c,t} = \text{ELU}(\mathbf{W}_c \mathbf{h}_t + \mathbf{a}_c) \quad (9a)$$

$$\mathbf{z}_{b,t} = \text{ELU}(\mathbf{W}_b \mathbf{h}_t + \mathbf{a}_b) \quad (9b)$$

$$\mathbf{z}_{e,t} = \text{ELU}(\mathbf{W}_e \mathbf{h}_t + \mathbf{a}_e) \quad (9c)$$

This groups together commonly found tasks in longitudinal studies, e.g. predicting trajectories of biomarker measurements, evaluating the risk of infection or developing additional comorbidities, and forecasting survival probabilities.

A prediction horizon τ is also concatenated with the longitudinal task-specific layers, so that the parameters for the predictive distributions at $t + \tau$ can be computed in the final layer, i.e. $\tilde{\mathbf{z}}_{c,t} = [\mathbf{z}_{c,t}, \tau]$ and $\tilde{\mathbf{z}}_{b,t} = [\mathbf{z}_{b,t}, \tau]$ for continuous and binary task layers respectively.

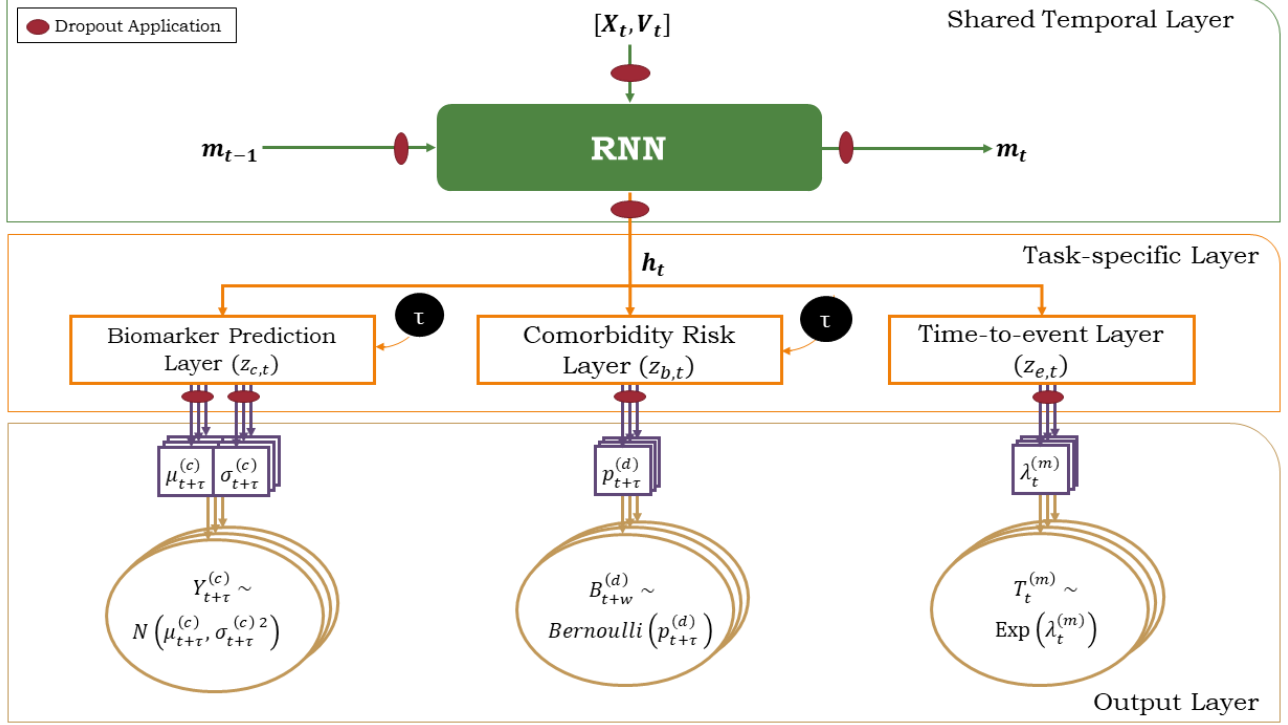


Fig. 2. Disease-Atlas Network Architecture

c) *Output Layer*: The final layer computes the parameter vectors of the predictive distribution, which are used to compute log likelihoods during training and dynamic predictions at runtime.

$$\mu_{t+\tau} = \mathbf{W}_\mu \mathbf{z}_{c,t} + \mathbf{a}_\mu \quad (10a)$$

$$\sigma_{t+\tau} = \text{Softplus}(\mathbf{W}_\sigma \tilde{\mathbf{z}}_{c,t} + \mathbf{a}_\sigma) \quad (10b)$$

$$\mathbf{p}_{t+\tau} = \text{Sigmoid}(\mathbf{W}_p \tilde{\mathbf{z}}_{b,t} + \mathbf{a}_p) \quad (10c)$$

$$\lambda_t = \text{Softplus}(\mathbf{W}_\lambda \mathbf{z}_{e,t} + \mathbf{a}_\lambda) \quad (10d)$$

Softplus activation functions are applied to $\sigma_{t+\tau}$ and $\mathbf{p}_{t+\tau}$ to ensure that we obtain valid (i.e. ≥ 0) standard deviations and binary probabilities. For simplicity, the exponential distribution is selected to model survival times, and predictive distributions can be expressed in a similar manner to that of Section III-A:

$$Y_{t+\tau}^{(c)} \sim N\left(\mu_{t+\tau}^{(c)}, \sigma_{t+\tau}^{(c)2}\right) \quad (11a)$$

$$B_{t+\tau}^{(d)} \sim \text{Bernoulli}\left(p_{t+\tau}^{(d)}\right) \quad (11b)$$

$$T_t^{(m)} \sim \text{Exponential}\left(\lambda_t^{(m)}\right) \quad (11c)$$

B. Multitask Learning

From the above, the negative log-likelihood of the data given the network is:

$$\begin{aligned} \mathcal{L}(\mathbf{W}) = & \sum_{i,t,w,k_c,k_b,m} - \left[\log f_c\left(Y_{i,t+\tau}^{(c)} | \mu_{t+\tau}^{(c)}, \sigma_{t+\tau}^{(c)2}, \mathbf{W}\right) \right. \\ & + \log f_b\left(B_{i,t+\tau}^{(d)} | p_{t+\tau}^{(d)}, \mathbf{W}\right) \\ & \left. + \log f_T\left(T_{i,t}^{(m)} | \lambda_t^{(m)}, \mathbf{W}\right) \right] \quad (12) \end{aligned}$$

Where $f_c(\cdot)$, $f_b(\cdot)$ are likelihood functions based on Equations 11 and \mathbf{W} collectively represents the weights and biases of the entire network. For survival times, $f_T(\cdot)$ is given as:

$$f_T\left(T | \lambda_t^{(m)}, \mathbf{W}\right) = S(T|t) \exp(-\lambda_t^{(m)} T)^{\delta_{i,T}} \quad (13)$$

Which corresponds to event-free survival until time T before encountering the event. While the negative log-likelihood can be directly optimized across tasks, the use of multitask learning can yield the following benefits:

a) *Better Survival Representations*: As shown in [21], multitask learning problems which have one main task of interest can weight the individual loss contributions of each subtask to favor representations for the main problem. For our

Algorithm 1 Training Disease-Atlas

Input: Data $\Omega = \{\Omega_1, \dots, \Omega_Q\}$, max iterations \mathcal{J}
Output: Calibrated network weights \mathbf{W}
for count=1 **to** \mathcal{J} **do**
 Get minibatch $\mathcal{M} \sim \gamma$ random samples from Ω
 Sample task loss function $l \sim \{l_c, l_b, l_T\}$
 Update $\mathbf{W} \leftarrow \text{Adam}(l, \mathcal{M})$, using feed-forward passes with dropout applied
end for

current architecture, where we group into similar tasks into task-specific layers, our loss function corresponds to:

$$\begin{aligned}
 L(\mathbf{W}) = & \underbrace{-\alpha_c \sum_{i,t,w,c} \log f_c \left(Y_{t+\tau}^{(c)} | \mathbf{W} \right)}_{\text{Continuous Longitudinal Loss } l_c} \\
 & - \underbrace{\alpha_b \sum_{i,t,w,d} \log f_b \left(B_{t+\tau}^{(d)} | \mathbf{W} \right)}_{\text{Binary Longitudinal Loss } l_b} \\
 & - \underbrace{\alpha_T \sum_{i,t,m} \log f_T \left(T_t^{(m)} | \mathbf{W} \right)}_{\text{Time-to-event Loss } l_T}
 \end{aligned} \quad (14)$$

Given that survival predictions are the primary focus of many longitudinal studies, we set $\alpha_c = \alpha_b = 1$ and include α_T as an additional hyperparameter to be optimized. To train the network, patient trajectories are subdivided into Q sets of $\Omega_q(i, \rho, \tau) = \{\mathbf{X}_{i,t:t+\rho}, \mathbf{Y}_{i,t+\tau}, \mathbf{T}_{\max,i}, \delta_i\}$, where ρ is the length of the covariate history to use in training trajectories up to a maximum of ρ_{\max} . Our procedure follows that of [25], as detailed in Algorithm 1.

b) Handling Irregularly Sampled Data: We address issues with irregular sampling by grouping variables that are measured together into the same task, and training the network with multitask learning. For instance, height, weight and BMI measurements are usually taken at the same time during follow-up, and can be grouped together in the same task. Given the completeness of the datasets we consider, we assume that task groupings match those defined by the task-specific layer of the network, and multitask learning is performed using Equation 14 and Algorithm 1.

We note, however, that in the extreme case where none of the trajectories are aligned, we can define each variable as a separate task with its own loss function l_* . Algorithm 1 then samples loss functions for one variable at a time, and the network is trained using only actual observations as target labels. This could reduce errors in cases where multiple sample rates exist and simple imputation is used, which might result in the multioutput networks replicating the imputation process instead of making true predictions.

C. Forecasting Disease Trajectories

Dynamic prediction involves 2 key elements - 1) calculating the expected longitudinal values and survival curves as described in Section III-B, and 2) computing uncertainty estimates. To obtain these measures, we apply the Monte-Carlo

dropout approach of [24] by approximating the posterior over network weights as:

$$p(V_{t+\tau}^{(k)} | \mathcal{F}_t) \approx \frac{1}{J} \sum_{j=1}^J p(V_{t+\tau}^{(k)} | \mathcal{F}_t, \hat{\mathbf{W}}_j) \quad (15)$$

Where we draw J samples $\hat{\mathbf{W}}_j$ using feed-forward passes through the network with the same dropout mask applied across time-steps. The samples obtained can then be used to compute expectations and uncertainty intervals for forecasts.

V. TESTS ON MEDICAL DATA

A. Overview of Datasets

The UK Cystic Fibrosis (CF) registry contains data obtained for a cohort of 10980 CF patients during annual follow ups between 2008-2015, with a total of 87 variables were associated with each patient across all years. In our investigations, we consider a joint model for 2 continuous lung function scores (FEV1 and Predicted FEV1), 20 comorbidity and infection risk (treated as binary longitudinal observations) and death as the event of interest, simultaneously forecasting them all at each time step. We refer the reader to Appendix A for a full breakdown of the dataset.

B. Method

We compared the Disease-Atlas (DA) against simpler neural networks i.e. LSTM and Multi-layer Perceptions (MLP), and traditional dynamic prediction methods, i.e. landmarking [1] and linear mixed effects models. The data was partitioned into 3 sets: a training set with 60% of the patients, a validation set with 20% and a testing set with the final 20%. Hyperparameter optimization was performed using random search (20 iterations), with full details in Appendix A. Models were compared using several metrics: Mean-Squared Error (MSE) for predictions of continuous longitudinal variables, and the area under the Receiver Operating Characteristic (AUROC) and Precision-Recall Curve (AUPRC) for binary variables and the event of interest, i.e. death. As metrics were computed using the mean estimates of MC dropout samples as predictions, with 100 samples used per timestep, we repeated the performance evaluation 3 times, reporting the means and standard deviations for mortality predictions in Table I. Note that this differs from the scores in Table II, which are reported as the average and standard deviations of AUROC and AUPRC across all binary predictions for the means of the first run.

a) Disease-Atlas: Through subsequent tests, we demonstrate the performance contributions of the different innovations of Disease-Atlas, namely the usage of multitask learning in the presence of irregular sampling (Section V-C), and the inclusion of the RNN in the base layer for temporal information (Section V-D). For the temporal layer, we consider the use of different RNNs (DA-RNN, DA-LSTM) or a single ELU layer (DA-NN).

b) Standard Neural Networks: Both the LSTM and MLP were taken to be benchmarks, and structured to produce the same output distribution parameters as the Disease-Atlas. These were optimized according to the multioutput loss function in Equation 12.

c) *Landmarking*: For consistency with other studies of Cystic Fibrosis [26], we use age as the time variable, and fit separate Cox regression models for patients in different age groups (< 25 , $25 - 50$, $50 - 75$ and > 75 years old). As data is left-truncated with respect to age, we use the entry-exit implementation of the Cox proportional hazards model implemented in [27]. To avoid issues with collinearity, we start with a preliminary feature selection step first - performing multi-step Cox regression on the validation dataset, and only retaining features with coefficient p-values < 0.1 .

d) *Linear Mixed Effects (LME) Sub-models*: With the computational limitations of standard joint models, direct application to our dataset, containing over 6,500 patients in the training set with 87 annual covariate measurements, proved to be infeasible. To put this into context, in our preliminary attempts to apply `JMbayes`, a popular R package for multivariate Bayesian Joint Models [28], to our dataset, the MCMC sampler ran for more than 7 hours without completion on an Intel i7-8700 CPU. In contrast, the optimal DA-RNN network, implemented in `Tensorflow` [29], was calibrated within 23 minutes on the same hardware.

As such, for each longitudinal variable, we tested our network against individual linear mixed effects models with random intercepts and slopes, which is akin to making predictions using the individual submodels directly. This form is in line with the models of FEV1, a measure of lung function, described in [30], [31] and [32]. For binary variables, we use the logit regression version of the LME model, as implemented in the `lme4` R package [33].

C. Evaluating Multitask Learning with Irregularly Sampled Data

To evaluate the effectiveness of multitask learning, we simulate irregular sampling by randomly removing all data points across each task (defined in Section IV-B) with a probability γ at every time step. For multivariate prediction, continuous-valued inputs were imputed using the mean value of the training set, while binary variables and indicators of death were set to 0. The networks were trained according to Section IV-B, and then evaluated on the complete test set based on 1) MSE for continuous variables, and 2) AUROC for binary/event predictions.

Figure 4 shows the outperformance of multitask learning, which has a lower MSE for FEV1 and higher AUROCs for comorbidity and mortality predictions as γ increases. The improvements are most pronounced for MSE, as FEV1 has values at every time step, as opposed to binary observations and occurrences of death which are relatively more infrequent in the dataset. This demonstrates the robustness of the model to irregular sampling, and provides a way for joint models to be used on datasets even under such conditions.

D. Performance vs Benchmarks

Given that survival analysis is the main task of interest, we start a comprehensive evaluation of across all benchmarks, computing a probability of the event of interest, i.e. death, at a given time step using $1 - S_i^{(m)}(\tau|t)$ from Equation 7.

Performance was compared on the basis of AUROC and AUPRC of mortality predictions at various horizons τ , and reported in Table I.

From the results, the DA-LSTM performed the best at short time horizons, with a one-step AUROC of 0.944 and AUPRC of 0.281, and both the DA-LSTM and DA-RNN outperforming other benchmarks across all time steps. The similarity between the results of the two RNN types can be attributed to the relatively small number of observations in time per patient (maximum of 8 observations between 2008-2015), and we can expect better performance for LSTMs over longer trajectories. In addition, we note the clear out-performance for neural networks over landmarking and joint models, indicating the benefits of more flexible techniques which do not require model specification.

Next, we evaluate the forecasting performance for longitudinal trajectories, zooming in on comparisons between DA-LSTM and LME. From Table II, the DA-LSTM outperforms the standard LME models across all MSE, AUROC and AUPRC metrics, demonstrating its usefulness as a method of scalable joint modeling.

VI. POTENTIAL USE CASE: PERSONALIZED SCREENING

A possible use case for the Disease-Atlas is in personalized screening, i.e. prescribing testing regimes and follow-up schedules that are tailored to the unique characteristics of a patient. [34] derive an optimal policy that balances the costs of screening, along with the risks of delaying the screening process. Their paper, however, has two important limitations: 1) it requires the evolution of the disease to be known, and 2) it requires an analytical expression for the cost of delay, which is often difficult to determine in practice. Disease-Atlas does not suffer from these limitations.

We illustrate how the Disease Atlas can be used for identifying screening profiles for Cystic Fibrosis patients. We use as an exemplar an actual patient from our test set who started to be seen in 2008 and is screened for Diabetes, a very important comorbidity affecting the treatment of patients.

Figure VI shows how the Disease Atlas can be used to design personalized screening policies. Using the Disease Atlas as applied from 2008-2010, we can record the “smoothed” estimate at each time step, i.e. $\hat{B}_i^{(d)}(0|t)$ as per Equation 6 and plotted in orange. To determine a patient’s future risk, we extrapolate in the usual way over various horizons τ , providing both the expected value and an uncertainty interval using the 5th and 95th percentiles of the MC dropout samples. From Figure 6, we see that the patient had a steady 18% increase in risk from 2008 to 2010, and will expect a further increase of 13% over the next 5 years. Informed by the Disease Atlas, the clinician may decide to prescribe additional tests for Diabetes, or increase the frequency of follow-up in the short-term to better monitor risks.

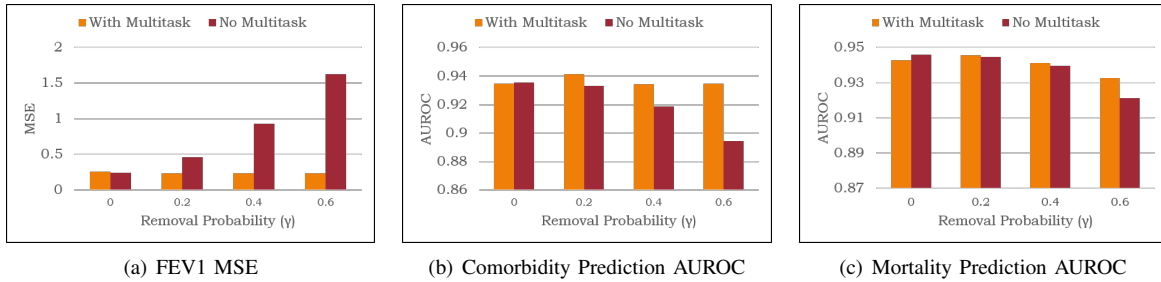


Fig. 3. Performance Comparison Between Multitask and Multioutput Networks

TABLE I
RESULTS OF MORTALITY PREDICTIONS FOR CYSTIC FIBROSIS (MEAN \pm S.D. ACROSS 3 RUNS)

	τ	DA-LSTM	DA-RNN	DA-NN	NN	LSTM	Landmarking
AUROC	1	0.944 (\pm 0.001)	0.942 (\pm 0.001)	0.923 (\pm 0.001)	0.941 (\pm 0.001)	0.934 (\pm 0.002)	0.824
	2	0.924 (\pm 0.002)	0.925 (\pm 0.001)	0.904 (\pm 0.001)	0.921 (\pm 0.001)	0.910 (\pm 0.001)	0.812
	3	0.912 (\pm 0.001)	0.910 (\pm 0.001)	0.886 (\pm 0.002)	0.906 (\pm 0.001)	0.894 (\pm 0.002)	0.825
	4	0.905 (\pm 0.002)	0.905 (\pm 0.001)	0.880 (\pm 0.000)	0.897 (\pm 0.000)	0.891 (\pm 0.002)	0.776
	5	0.897 (\pm 0.001)	0.900 (\pm 0.002)	0.871 (\pm 0.002)	0.892 (\pm 0.001)	0.886 (\pm 0.002)	0.765
AUPRC	1	0.281 (\pm 0.008)	0.273 (\pm 0.007)	0.158 (\pm 0.002)	0.205 (\pm 0.008)	0.143 (\pm 0.008)	0.161
	2	0.190 (\pm 0.010)	0.188 (\pm 0.010)	0.151 (\pm 0.002)	0.171 (\pm 0.007)	0.121 (\pm 0.011)	0.082
	3	0.118 (\pm 0.004)	0.099 (\pm 0.004)	0.097 (\pm 0.001)	0.091 (\pm 0.005)	0.091 (\pm 0.007)	0.085
	4	0.104 (\pm 0.002)	0.109 (\pm 0.002)	0.085 (\pm 0.003)	0.097 (\pm 0.002)	0.083 (\pm 0.003)	0.062
	5	0.101 (\pm 0.001)	0.100 (\pm 0.002)	0.093 (\pm 0.001)	0.092 (\pm 0.005)	0.094 (\pm 0.004)	0.058

TABLE II
RESULTS OF LONGITUDINAL PREDICTIONS FOR CYSTIC FIBROSIS (SINGLE RUN)

	τ	MSE		AUROC [Ave. \pm S.D.]		AUPRC [Ave. \pm S.D.]	
		FEV1	Pred. FEV1	Comorbidities	Infections	Comorbidities	Infections
DA-LSTM	1	0.186	125.742	0.978 (\pm 0.011)	0.932 (\pm 0.043)	0.836 (\pm 0.170)	0.579 (\pm 0.233)
	2	0.206	145.669	0.945 (\pm 0.032)	0.885 (\pm 0.030)	0.765 (\pm 0.168)	0.432 (\pm 0.254)
	3	0.295	198.444	0.898 (\pm 0.047)	0.827 (\pm 0.061)	0.655 (\pm 0.130)	0.385 (\pm 0.264)
	4	0.389	256.973	0.833 (\pm 0.084)	0.743 (\pm 0.075)	0.519 (\pm 0.160)	0.321 (\pm 0.259)
	5	0.471	308.318	0.805 (\pm 0.074)	0.693 (\pm 0.111)	0.438 (\pm 0.153)	0.301 (\pm 0.243)
LME	1	0.553	368.61	0.699 (\pm 0.148)	0.673 (\pm 0.069)	0.176 (\pm 0.088)	0.161 (\pm 0.176)
	2	0.593	411.162	0.694 (\pm 0.139)	0.651 (\pm 0.060)	0.180 (\pm 0.089)	0.157 (\pm 0.181)
	3	0.641	451.754	0.685 (\pm 0.140)	0.631 (\pm 0.072)	0.185 (\pm 0.090)	0.160 (\pm 0.186)
	4	0.695	490.118	0.681 (\pm 0.132)	0.607 (\pm 0.077)	0.187 (\pm 0.091)	0.159 (\pm 0.188)
	5	0.75	519.652	0.673 (\pm 0.130)	0.580 (\pm 0.082)	0.188 (\pm 0.093)	0.155 (\pm 0.186)

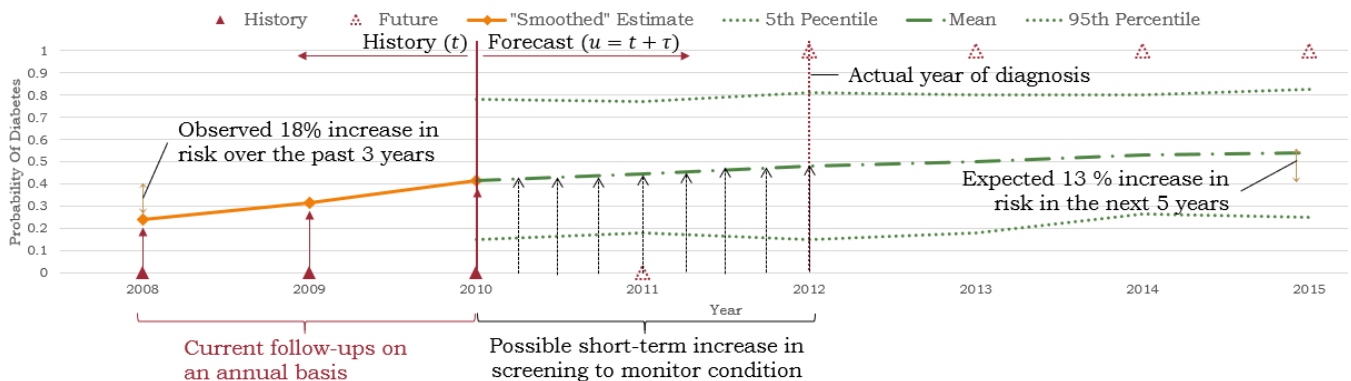


Fig. 4. Using Disease-Atlas for Personalized Screening

REFERENCES

- [1] H. van Houwelingen and H. Putter, *Dynamic Prediction in Clinical Survival Analysis*. Boca Raton, FL, USA: CRC Press, Inc., 2011.
- [2] D. Rizopoulos, G. Molenberghs, and E. M. Lesaffre, “Dynamic predictions with time-dependent covariates in survival analysis using joint modeling and landmarking,” *Biometrical Journal*, vol. 59, no. 6, pp. 1521–4036, 2017.
- [3] A. B. Jensen, P. L. Moseley, T. I. Oprea, S. G. Ellese, R. Eriksson, H. Schmock, P. B. Jensen, L. Juh, Jensen, and S. Brunak, “Temporal disease trajectories condensed from population-wide registry data covering 6.2 million patients,” *Nature Communications*, vol. 5, no. 4022, 2014.
- [4] V. Kannan, N. A. Kiani, F. Piehl, and J. Tegner, “A minimal unified model of disease trajectories captures hallmarks of multiple sclerosis,” *Mathematical Biosciences*, vol. 289, pp. 1 – 8, 2017.
- [5] C. Farmer, E. Fenu, N. O’Flynn, and B. Guthrie, “Clinical assessment and management of multimorbidity: summary of nice guidance,” *BMJ*, vol. 354, 2016.
- [6] X. Xu, G. D. Mishra, and M. Jones, “Evidence on multimorbidity from definition to intervention: An overview of systematic reviews,” *Ageing Research Reviews*, vol. 37, pp. 53 – 68, 2017.
- [7] G. L. Hickey, P. Philipson, A. Jorgensen, and R. Kolamunnage-Dona, “Joint modelling of time-to-event and multivariate longitudinal outcomes: recent developments and issues,” *BMC Medical Research Methodology*, vol. 16, no. 1, p. 117, Sep 2016.
- [8] J. G. Ibrahim, H. Chu, and L. M. Chen, “Basic concepts and methods for joint models of longitudinal and survival data,” *Journal of Clinical Oncology*, vol. 28, no. 16, p. 27962801, 2010.
- [9] J. W. Hogan and N. M. Laird, “Increasing efficiency from censored survival data by using random effects to model longitudinal covariates,” *Statistical Methods in Medical Research*, vol. 7, no. 1, pp. 28–48, 1998.
- [10] A. M. Alaa and M. van der Schaar, “Deep multi-task gaussian processes for survival analysis with competing risks,” in *Advances in Neural Information Processing Systems*, ser. NIPS 2017, 2017.
- [11] R. Ranganath, A. Perotte, N. Elhadad, and D. Blei, “Deep survival analysis,” in *Proceedings of the 1st Machine Learning for Healthcare Conference*, ser. Proceedings of Machine Learning Research, vol. 56, 18–19 Aug 2016, pp. 101–114.
- [12] D. Rizopoulos, L. A. Hatfield, B. P. Carlin, and J. J. M. Takkenberg, “Combining dynamic predictions from joint models for longitudinal and time-to-event data using bayesian model averaging,” *Journal of the American Statistical Association*, vol. 109, no. 508, pp. 1385–1397, 2014.
- [13] J. Barrett, P. Diggle, R. Henderson, and D. Taylor-Robinson, “Joint modelling of repeated measurements and time-to-event outcomes: flexible model specification and exact likelihood inference,” *Journal of the Royal Statistical Society: Series B (Statistical Methodology)*, vol. 77, no. 1, pp. 131–148, 2015.
- [14] E. Waldmann, D. Taylor-Robinson, N. Klein, T. Kneib, T. Pressler, M. Schmid, and A. Mayr, “Boosting joint models for longitudinal and time-to-event data,” *Biometrical Journal*, vol. 59, no. 6, pp. 1104–112, 2017.
- [15] J. Futoma, M. Sendak, C. B. Cameron, and K. Heller, “Scalable joint modeling of longitudinal and point process data for disease trajectory prediction and improving management of chronic kidney disease,” in *Proceedings of the Thirty-Second Conference on Uncertainty in Artificial Intelligence*, ser. UAI’16, 2016, pp. 222–231.
- [16] J. Barrett and L. Su, “Dynamic predictions using flexible joint models of longitudinal and timetoevent data,” *Statistics in Medicine*, vol. 36, no. 9, pp. 1447–1460, Apr. 2017.
- [17] M. Luck, T. Sylvain, H. Cardinal, A. Lodi, and Y. Bengio, “Deep learning for patient-specific kidney graft survival analysis,” *CoRR*, vol. abs/1705.10245, 2017. [Online]. Available: <http://arxiv.org/abs/1705.10245>
- [18] C. Lee, W. R. Zame, J. Yoon, and M. van der Schaar, “Deephit: A deep learning approach to survival analysis with competing risks,” in *AAAI*, 2018.
- [19] J. Katzman, U. Shaham, J. Bates, A. Cloninger, T. Jiang, and Y. Kluger, “Deepsurv: Personalized treatment recommender system using a cox proportional hazards deep neural network,” in *Proceedings of the 33rd International Conference on International Conference on Machine Learning - Volume 48*, ser. ICML 2016, 2016.
- [20] R. G. Krishnan, U. Shalit, and D. Sontag, “Deep kalman filters,” *CoRR*, vol. abs/1511.05121, 2017. [Online]. Available: <https://arxiv.org/abs/1511.05121>
- [21] F. Li, L. Tran, K.-H. Thung, S. Ji, D. Shen, and J. Li, “A robust deep model for improved classification of ad/mci patients,” *IEEE journal of biomedical and health informatics*, vol. 19, no. 5, pp. 1610–1616, 2015.
- [22] H. Harutyunyan, H. Khachatrian, D. C. Kale, and A. Galstyan, “Multitask learning and benchmarking with clinical time series data,” *CoRR*, vol. abs/1703.07771, 2017. [Online]. Available: <https://arxiv.org/abs/1703.07771>
- [23] J. Ibrahim, M. Chen, and D. Sinha, “Bayesian methods for joint modeling of longitudinal and survival data with applications to cancer vaccine trials,” *Statistica Sinica*, vol. 14, no. 3, pp. 863–883, 7 2004.
- [24] Y. Gal and Z. Ghahramani, “A theoretically grounded application of dropout in recurrent neural networks,” in *Advances in Neural Information Processing Systems*, ser. NIPS 2016, 2016.
- [25] R. Collobert and J. Weston, “A unified architecture for natural language processing: Deep neural networks with multitask learning,” in *Proceedings of the 25th International Conference on Machine Learning*, ser. ICML 2008, 2008, pp. 160–167.
- [26] T. MacKenzie, A. H. Gifford, K. A. Sabadosa, H. B. Quinton, E. A. Knapp, C. H. Goss, and B. C. Marshall, “Longevity of patients with cystic fibrosis in 2000 to 2010 and beyond: Survival analysis of the cystic fibrosis foundation patient registry,” *I Annals of internal medicine*, vol. 161, no. 4, pp. 233–241, 2014.
- [27] T. M. Therneau, *A Package for Survival Analysis in S*, 2015, version 2.38. [Online]. Available: <https://CRAN.R-project.org/package=survival>
- [28] D. Rizopoulos, “The R package JMbayes for fitting joint models for longitudinal and time-to-event data using mcmc,” *Journal of Statistical Software*, vol. 72, no. 7, pp. 1–45, 2016.
- [29] M. Abadi, A. Agarwal, P. Barham, E. Brevdo, Z. Chen, C. Citro, G. S. Corrado, A. Davis, J. Dean, M. Devin, S. Ghemawat, I. Goodfellow, A. Harp, G. Irving, M. Isard, Y. Jia, R. Jozefowicz, L. Kaiser, M. Kudlur, J. Levenberg, D. Mané, R. Monga, S. Moore, D. Murray, C. Olah, M. Schuster, J. Shlens, B. Steiner, I. Sutskever, K. Talwar, P. Tucker, V. Vanhoucke, V. Vasudevan, F. Viégas, O. Vinyals, P. Warden, M. Wattenberg, M. Wicke, Y. Yu, and X. Zheng, “TensorFlow: Large-scale machine learning on heterogeneous systems,” 2015, software available from tensorflow.org. [Online]. Available: <https://www.tensorflow.org/>
- [30] M. van Horck, B. Winkens, G. Wesseling, D. van Vliet, K. van de Kant, S. Vaassen, K. de Winter-de Groot, I. de Vreede, Q. Jbsis, and E. Dompeling, “Early detection of pulmonary exacerbations in children with cystic fibrosis by electronic home monitoring of symptoms and lung function,” *Scientific Reports*, vol. 7, no. 1, 2017.
- [31] C. Van Diemen, D. Postma, M. Siedlinski, A. Blokstra, H. Smit, and H. Boezen, “Genetic variation in timp1 but not mmprs predict excess fev1 decline in two general population-based cohorts,” *Respiratory Research*, vol. 12, no. 1, 2011.
- [32] D. A. Stern, W. J. Morgan, A. L. Wright, S. Guerra, and F. D. Martinez, “Poor airway function in early infancy and lung function by age 22 years: a non-selective longitudinal cohort study,” *Lancet*, vol. 370, 2007.
- [33] D. Bates, M. Mächler, B. Bolker, and S. Walker, “Fitting linear mixed-effects models using lme4,” *Journal of Statistical Software*, vol. 67, no. 1, pp. 1–48, 2015.
- [34] K. Ahuja, W. Zame, and M. van der Schaar, “Dpscreen: Dynamic personalized screening,” in *Advances in Neural Information Processing Systems*, ser. NIPS 2017, I. Guyon, U. V. Luxburg, S. Bengio, H. Wallach, R. Fergus, S. Vishwanathan, and R. Garnett, Eds., 2017, pp. 1321–1332.

APPENDIX

This appendix contains supplementary information on the tests conducted on data from the UK Cystic Fibrosis Trust.

A. Details on Dataset

The UK Cystic Fibrosis (CF) registry contains data obtained for a cohort of 10980 CF patients during annual follow ups between 2008-2015, with a total of 87 variables that were associated with each patient across all years. This includes demographic information (e.g. age, height, weight, BMI), genetic information, treatments received, metrics for lung function (FEV1 and Predicted FEV1), comorbidities observed, and any bacterial infections developed. In our investigations, we consider a joint model for the 2 continuous lung function scores (FEV1 and Predicted FEV1), 20 binary longitudinal variables of comorbidity and infection, along with death as the event of interest.

A full description of the jointly-modeled longitudinal and time-to-event datasets can be found in Table III.

B. Hyperparameter Optimization

Hyperparameter optimization was conducted using 20 iterations of random search, with the search space documented in Table IV. Please note that the RNN state size was defined relative to the number of input features (L). The task specific layers were also size in relation to the RNN state size, and defined to be $(\text{state size} + \text{task output size}) / 2$. This was done to ensure that we had a principled way of sizing the task-specific layer relative to state size and outputs, without having to add on too many additional hyper-parameters (i.e. one per task-specific layer). In addition, α_T was defined in relation to the number of longitudinal variables (K). All neural networks were trained to convergence, as determined by the log-likelihoods evaluated on the validation data, or up to a maximum of 50 epochs.

The final parameters obtained for each network can be found in Table V.

C. Additional Results

To supplement the results in the test section of the main report, a detailed breakdown of the prediction results for binary longitudinal variables can be found in Table VI and VII for DA-LSTM and Linear Mixed Effects Models respectively. For the DA-LSTM, due to the randomness present in the MC dropout procedure, the performance evaluation was repeated 3 times with the means and standard deviations reported in the tables. The results also demonstrate the clear outperformance of the deep neural network over standard linear mixed effects models in both AUROC and AUPRC terms.

D. Acknowledgments

We would like to thank the UK Cystic Fibrosis Trust for providing us access to the data from the CF registry, which was used extensively in the analysis performed in this report.

TABLE III
DESCRIPTION OF LONGITUDINAL AND TIME-TO-EVENT DATA FOR CF

		Type	% Patients Observed	Mean	S.D.	Min	Max
Event	Death	Binary (Event)	4.70%	0.008	0.087	0.000	1.000
Biomarkers	FEV1	Continuous	100.00%	2.176	0.914	0.090	6.250
	Predicted FEV1	Continuous	100.00%	72.109	22.404	8.950	197
Comorbidities	Liver Disease	Binary	20.80%	0.128	0.334	0.000	1.000
	Asthma	Binary	22.96%	0.146	0.353	0.000	1.000
	Arthropathy	Binary	9.50%	0.050	0.218	0.000	1.000
	Bone fracture	Binary	1.94%	0.007	0.081	0.000	1.000
	Raised Liver Enzymes	Binary	23.91%	0.114	0.318	0.000	1.000
	Osteopenia	Binary	20.37%	0.114	0.318	0.000	1.000
	Osteoporosis	Binary	9.58%	0.051	0.219	0.000	1.000
	Hypertension	Binary	3.30%	0.020	0.139	0.000	1.000
	Diabetes	Binary	24.56%	0.167	0.373	0.000	1.000
Bacterial Infections	Burkholderia Cepacia	Binary	5.59%	0.034	0.181	0.000	1.000
	Pseudomonas Aeruginosa	Binary	65.18%	0.407	0.491	0.000	1.000
	Haemophilus Influenza	Binary	30.55%	0.091	0.288	0.000	1.000
	Aspergillus	Binary	29.29%	0.110	0.313	0.000	1.000
	NTM	Binary	6.38%	0.019	0.136	0.000	1.000
	Ecoli	Binary	5.32%	0.012	0.111	0.000	1.000
	Klebsiella Pneumoniae	Binary	4.93%	0.010	0.101	0.000	1.000
	Gram-Negative	Binary	3.78%	0.008	0.089	0.000	1.000
	Xanthomonas	Binary	13.18%	0.043	0.202	0.000	1.000
	Staphylococcus Aureus	Binary	52.59%	0.244	0.429	0.000	1.000
	ALCA	Binary	5.06%	0.020	0.138	0.000	1.000

TABLE IV
HYPER-PARAMETER SELECTION RANGE FOR RANDOM SEARCH

Hyper-parameter Selection Range	
Max Number of Epochs	50
RNN State Size	0.5L, 1L, 1.5L, 2L, 2.5L, 3.0L
α_T	K, 2K, 3K, 4K, 5K
Max Gradient Norm	0.5, 1.0, 1.5, 2.0
Learning Rate	1e-2, 5e-2, 1e-3, 5e-3, 1e-4
Minibatch Size	32, 64, 128, 256
Dropout Rate	0.1, 0.15, 0.2, 0.25, 0.3, 0.35, 0.4, 0.45, 0.5

TABLE V
HYPER-PARAMETERS SELECTED FOR CF TESTS

	State Size	Minibatch Size	Learning Rate	Max Gradient Norm	Dropout Rate	α_T
DA-RNN	2L	256	1.00E-04	1.5	0.5	3K
DA-LSTM	3L	256	1.00E-04	1.5	0.45	3K
DA-NN	2L	128	1.00E-02	1.5	0.1	4K
Standard NN	1.5L	64	1.00E-03	1	0.45	1K
Standard LSTM	1L	32	1.00E-03	1.5	0.4	4K

TABLE VI
AUROC FOR COMORBIDITY AND INFECTION PREDICTIONS FOR CF DATASET (MEAN \pm S.D. ACROSS 3 RUNS)

DA-LSTM	1	2	3	4	5
Comorbidities					
Liver Disease	0.978 (\pm 0.000)	0.945 (\pm 0.001)	0.891 (\pm 0.001)	0.826 (\pm 0.001)	0.769 (\pm 0.001)
Asthma	0.985 (\pm 0.000)	0.949 (\pm 0.000)	0.905 (\pm 0.001)	0.844 (\pm 0.001)	0.804 (\pm 0.001)
Arthropathy	0.989 (\pm 0.000)	0.963 (\pm 0.000)	0.926 (\pm 0.001)	0.896 (\pm 0.000)	0.839 (\pm 0.001)
Bone fracture	0.964 (\pm 0.003)	0.859 (\pm 0.004)	0.831 (\pm 0.005)	0.649 (\pm 0.006)	0.729 (\pm 0.007)
Raised Liver Enzymes	0.960 (\pm 0.001)	0.929 (\pm 0.001)	0.812 (\pm 0.001)	0.749 (\pm 0.002)	0.694 (\pm 0.002)
Osteopenia	0.974 (\pm 0.000)	0.954 (\pm 0.001)	0.909 (\pm 0.001)	0.881 (\pm 0.001)	0.855 (\pm 0.001)
Osteoporosis	0.986 (\pm 0.000)	0.969 (\pm 0.000)	0.936 (\pm 0.001)	0.892 (\pm 0.001)	0.865 (\pm 0.001)
Hypertension	0.996 (\pm 0.000)	0.984 (\pm 0.001)	0.974 (\pm 0.001)	0.949 (\pm 0.001)	0.936 (\pm 0.001)
Diabetes	0.973 (\pm 0.001)	0.951 (\pm 0.001)	0.924 (\pm 0.001)	0.880 (\pm 0.001)	0.852 (\pm 0.000)
Infections					
Burkholderia Cepacia	0.983 (\pm 0.001)	0.948 (\pm 0.001)	0.945 (\pm 0.001)	0.896 (\pm 0.002)	0.851 (\pm 0.002)
Pseudomonas Aeruginosa	0.903 (\pm 0.001)	0.876 (\pm 0.001)	0.847 (\pm 0.001)	0.817 (\pm 0.001)	0.799 (\pm 0.001)
Haemophilus Influenza	0.886 (\pm 0.002)	0.857 (\pm 0.001)	0.805 (\pm 0.001)	0.747 (\pm 0.001)	0.745 (\pm 0.001)
Aspergillus	0.944 (\pm 0.000)	0.873 (\pm 0.001)	0.855 (\pm 0.002)	0.729 (\pm 0.001)	0.708 (\pm 0.001)
NTM	0.948 (\pm 0.001)	0.863 (\pm 0.002)	0.880 (\pm 0.001)	0.721 (\pm 0.002)	0.670 (\pm 0.003)
Ecoli	0.954 (\pm 0.002)	0.918 (\pm 0.003)	0.699 (\pm 0.009)	0.597 (\pm 0.007)	0.411 (\pm 0.007)
Klebsiella Pneumoniae	0.976 (\pm 0.000)	0.917 (\pm 0.002)	0.854 (\pm 0.005)	0.654 (\pm 0.005)	0.715 (\pm 0.010)
Gram-Negative	0.827 (\pm 0.009)	0.836 (\pm 0.009)	0.765 (\pm 0.004)	0.762 (\pm 0.009)	0.597 (\pm 0.005)
Xanthomonas	0.948 (\pm 0.002)	0.878 (\pm 0.002)	0.801 (\pm 0.001)	0.746 (\pm 0.003)	0.693 (\pm 0.002)
Staphylococcus Aureus	0.935 (\pm 0.001)	0.880 (\pm 0.002)	0.795 (\pm 0.001)	0.713 (\pm 0.001)	0.669 (\pm 0.001)
ALCA	0.949 (\pm 0.001)	0.889 (\pm 0.002)	0.851 (\pm 0.001)	0.789 (\pm 0.005)	0.767 (\pm 0.004)
LME					
Comorbidities					
Liver Disease	0.634	0.622	0.619	0.607	0.602
Asthma	0.701	0.671	0.649	0.622	0.597
Arthropathy	0.761	0.755	0.755	0.757	0.749
Bone Fracture	0.344	0.379	0.378	0.413	0.411
Raised Liver Enzymes	0.622	0.608	0.589	0.584	0.594
Osteopenia	0.774	0.767	0.761	0.758	0.746
Osteoporosis	0.801	0.794	0.781	0.772	0.76
Hypertension	0.894	0.891	0.893	0.893	0.889
Diabetes	0.76	0.754	0.739	0.723	0.709
Infections					
Burkholderia Cepacia	0.636	0.638	0.63	0.622	0.613
Pseudomonas Aeruginosa	0.744	0.735	0.727	0.713	0.692
Haemophilus Influenza	0.698	0.712	0.722	0.715	0.685
Aspergillus	0.716	0.689	0.662	0.622	0.603
NTM	0.709	0.686	0.678	0.633	0.586
Ecoli	0.729	0.604	0.507	0.444	0.389
Klebsiella Pneumoniae	0.777	0.73	0.706	0.67	0.624
Gram-Negative	0.533	0.55	0.53	0.518	0.489
Xanthomonas	0.628	0.613	0.604	0.611	0.603
Staphylococcus Aureus	0.607	0.589	0.577	0.561	0.542
ALCA	0.624	0.613	0.598	0.572	0.552

TABLE VII
AUPRC FOR COMORBIDITY AND INFECTION PREDICTIONS FOR CF DATASET (MEAN \pm S.D. ACROSS 3 RUNS)

DA-LSTM	1	2	3	4	5
Comorbidities					
Liver Disease	0.910 (\pm 0.003)	0.839 (\pm 0.002)	0.697 (\pm 0.007)	0.608 (\pm 0.006)	0.507 (\pm 0.006)
Asthma	0.937 (\pm 0.001)	0.845 (\pm 0.002)	0.759 (\pm 0.004)	0.628 (\pm 0.006)	0.548 (\pm 0.004)
Arthropathy	0.914 (\pm 0.004)	0.830 (\pm 0.004)	0.682 (\pm 0.009)	0.536 (\pm 0.007)	0.385 (\pm 0.011)
Bone fracture	0.329 (\pm 0.028)	0.266 (\pm 0.032)	0.319 (\pm 0.016)	0.106 (\pm 0.007)	0.080 (\pm 0.005)
Raised Liver Enzymes	0.858 (\pm 0.004)	0.773 (\pm 0.003)	0.561 (\pm 0.005)	0.425 (\pm 0.008)	0.343 (\pm 0.006)
Osteopenia	0.870 (\pm 0.003)	0.818 (\pm 0.003)	0.701 (\pm 0.003)	0.608 (\pm 0.007)	0.528 (\pm 0.006)
Osteoporosis	0.886 (\pm 0.003)	0.829 (\pm 0.003)	0.636 (\pm 0.008)	0.457 (\pm 0.011)	0.372 (\pm 0.008)
Hypertension	0.876 (\pm 0.010)	0.828 (\pm 0.003)	0.767 (\pm 0.002)	0.647 (\pm 0.006)	0.537 (\pm 0.003)
Diabetes	0.898 (\pm 0.003)	0.839 (\pm 0.006)	0.796 (\pm 0.004)	0.690 (\pm 0.003)	0.670 (\pm 0.002)
Infections					
Burkholderia Cepacia	0.891 (\pm 0.004)	0.811 (\pm 0.013)	0.804 (\pm 0.006)	0.724 (\pm 0.005)	0.589 (\pm 0.009)
Pseudomonas Aeruginosa	0.846 (\pm 0.001)	0.821 (\pm 0.002)	0.810 (\pm 0.002)	0.796 (\pm 0.003)	0.797 (\pm 0.003)
Haemophilus Influenza	0.460 (\pm 0.002)	0.366 (\pm 0.001)	0.266 (\pm 0.003)	0.249 (\pm 0.002)	0.287 (\pm 0.003)
Aspergillus	0.683 (\pm 0.005)	0.468 (\pm 0.010)	0.505 (\pm 0.004)	0.364 (\pm 0.005)	0.362 (\pm 0.001)
NTM	0.524 (\pm 0.012)	0.188 (\pm 0.004)	0.313 (\pm 0.004)	0.213 (\pm 0.005)	0.196 (\pm 0.006)
Ecoli	0.518 (\pm 0.007)	0.241 (\pm 0.013)	0.082 (\pm 0.016)	0.029 (\pm 0.002)	0.008 (\pm 0.001)
Klebsiella Pneumoniae	0.397 (\pm 0.020)	0.184 (\pm 0.005)	0.068 (\pm 0.006)	0.013 (\pm 0.001)	0.017 (\pm 0.001)
Gram-Negative	0.037 (\pm 0.001)	0.047 (\pm 0.008)	0.034 (\pm 0.002)	0.032 (\pm 0.001)	0.021 (\pm 0.000)
Xanthomonas	0.547 (\pm 0.007)	0.404 (\pm 0.009)	0.327 (\pm 0.006)	0.223 (\pm 0.003)	0.190 (\pm 0.007)
Staphylococcus Aureus	0.833 (\pm 0.002)	0.748 (\pm 0.004)	0.630 (\pm 0.004)	0.555 (\pm 0.003)	0.516 (\pm 0.003)
ALCA	0.634 (\pm 0.015)	0.473 (\pm 0.008)	0.394 (\pm 0.007)	0.337 (\pm 0.004)	0.333 (\pm 0.004)
LME					
Comorbidities					
Liver Disease	0.181	0.186	0.197	0.2	0.207
Asthma	0.272	0.261	0.258	0.245	0.24
Arthropathy	0.134	0.142	0.148	0.155	0.154
Bone Fracture	0.006	0.007	0.007	0.009	0.01
Raised Liver Enzymes	0.163	0.16	0.156	0.157	0.172
Osteopenia	0.245	0.255	0.266	0.278	0.28
Osteoporosis	0.144	0.149	0.151	0.146	0.134
Hypertension	0.123	0.13	0.141	0.142	0.142
Diabetes	0.319	0.334	0.342	0.348	0.356
Infections					
Burkholderia Cepacia	0.054	0.058	0.056	0.056	0.062
Pseudomonas Aeruginosa	0.636	0.641	0.65	0.655	0.649
Haemophilus Influenza	0.181	0.204	0.233	0.231	0.202
Aspergillus	0.22	0.22	0.218	0.212	0.216
NTM	0.076	0.068	0.072	0.062	0.041
Ecoli	0.098	0.037	0.025	0.011	0.005
Klebsiella Pneumoniae	0.051	0.037	0.026	0.025	0.027
Gram-Negative	0.009	0.01	0.012	0.012	0.015
Xanthomonas	0.079	0.079	0.087	0.092	0.098
Staphylococcus Aureus	0.336	0.337	0.344	0.347	0.345
ALCA	0.037	0.04	0.037	0.04	0.047